DOI: 10.1002/chem.200600055

Significantly Accelerated Direct Electron-Transfer Kinetics of Hemoglobin in a C_{60}-MWCNT Nanocomposite Film

Hua Zhang,[a] Louzhen Fan,*[a] and Shihe Yang*[b]

Abstract: The direct electrochemistry of hemoglobin (Hb) was studied in a novel all-carbon nanocomposite film of C_{60}-MWCNT (MWCNT = multiple-walled carbon nanotube) and compared with that in bare MWCNT film. The heterogeneous electron-transfer rate constant k_s of Hb/C_{60}-MWCNT was determined to be 0.39 s^{-1}, which is more than one order of magnitude greater than that of Hb/MWCNT (0.03 s^{-1}). The significantly accelerated electron-transfer kinetics are attributed to the mediator role played by C_{60}, which is finely dispersed on the MWCNT surfaces. The excellent stability of Hb/C_{60}-MWCNT was established and its potential application towards the electrocatalytic reduction of O_2 was demonstrated.

Keywords: absorption · carbon nanotubes · electrochemistry · hemoglobin · nanocomposite films

Introduction

As new members of the carbon family, C_{60} and carbon nanotubes have attracted the interest of scientists on account of their fascinating structures and unusual properties. An interesting range of biological activities of fullerenes and fullerene derivatives has been revealed in recent investigations.[1–5] At the same time, many applications of carbon nanotubes have been reported, such as chemical sensors,[6–10] field emission materials,[11] and tips in scanning probe microscopy.[12,13] In particular, benefiting from both their favorable electrocatalytic characteristics and their small size, carbon nanotubes are an attractive material in bioelectrochemistry and as such, the performance of carbon nanotube-modified electrodes has been shown to be superior to that of other carbon electrodes.[14]

The electrochemical study of redox proteins has been an active area of research in recent years.[15,16] Because of its known structure and commercial availability, hemoglobin (Hb) is a model system of heme proteins in terms of electrochemistry. The study of the direct electrochemistry of Hb can facilitate the study of enzyme electron transfer in biological systems and provide a platform for fabricating biosensors. However, hemoglobin contains four electroactive iron heme groups and has a molar mass of approximately 67 000 g mol^{-1}. In addition, the redox centers (heme groups) are deeply immersed in the protein body, so it is difficult for Hb to exchange electrons with the electrode surface directly.[17–19] Presently, there is interest in enhancing the electron transfer of hemoglobin by preparing all kinds of modified electrodes, for example, polymer films[20] and egg-phosphatidycholine films[21]. Carbon nanotubes have also been applied for this purpose because of their remarkable electrocatalytic properties.[22] As an excellent electron acceptor, C_{60} could be dispersed in matrices, such as carbon nanotubes, to facilitate electron transfer. This indeed has been achieved by embedding fullerenes in didodecyldimethylammonium bromide (DDAB) membranes.[23]

Recently, we created a novel C_{60}-MWCNT nanocomposite film by an electrochemical means.[24] The electrochemistry of the nanocomposite film in an organic solution was found to be similar to that of homogeneously dissolved C_{60}, but with signatures of bare MWCNTs in term of a monotonic charge injection. As a further significant step, we used the C_{60}-MWCNT nanocomposite film to modify a glassy carbon (GC) electrode and studied extensively the direct electrochemical behavior of Hb on this surface-modified electrode in aqueous solutions.[25,26] This paper reports the main results of these investigations, including 1) an increase by one order

[a] H. Zhang, Dr. L. Fan
Department of Chemistry, Beijing Normal University
Beijing, China, 100875
Fax: (+86) 10-5880-2075
E-mail: lzfan@bnu.edu.cn

[b] Prof. S. Yang
Department of Chemistry
The Hong Kong University of Science and Technology
Clear Water Bay, Kowloon (Hong Kong)
Fax: (+852) 2358-1594
E-mail: chsyang@ust.hk

of magnitude of the heterogeneous electron-transfer rate constant of Hb/C_{60}-MWCNT relative to that of Hb/MWCNT; and 2) an excellent electrocatalytic activity of Hb/C_{60}-MWCNT for the reduction of O_2.

Results and discussion

Electrochemical behavior of Hb on C_{60}-MWCNT nanocomposite film electrode: The C_{60}-MWCNT nanocomposite film is known to exhibit very stable electrochemical behavior in organic solution, as reported previously.[24] Here, we explore its novel electrochemical properties in aqueous solutions. Figure 1 displays typical cyclic voltammograms (CVs) of a

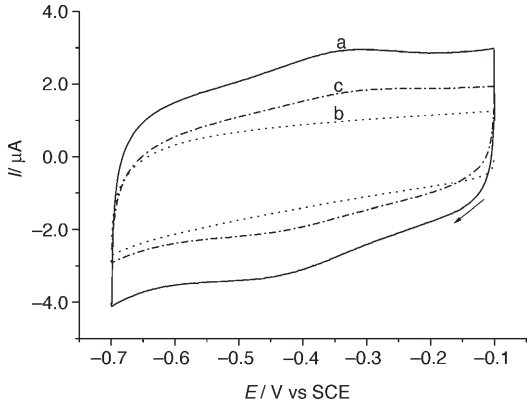

Figure 1. Cyclic voltammograms of a C_{60}-MWCNT film (a,b) and a MWCNT film (c) on a GC electrode in pH 7.0 phosphate buffer solution with 5×10^{-5} M Hb (a,c) and without Hb (b). Scan rate: 0.01 V s^{-1}.

C_{60}-MWCNT film on a GC electrode in pH 7.0 phosphate buffer solution with 5×10^{-5} M Hb (curve a) and without Hb (curve b). In curve a, a pair of well-defined redox peaks at −0.403 and −0.362 V (vs saturated calomel electrode (SCE)) is seen, whereas no peak exists in curve b within the same potential range. Evidently, the peaks in curve a arise from the protein adsorbed on the C_{60}-MWCNT film. For comparison, the CVs of a bare MWCNT film on a GC electrode in pH 7.0 phosphate buffer solution with 5×10^{-5} M Hb is also shown in Figure 1 (curve c). In this case, the peak currents are much smaller than those with the C_{60}-MWCNT film. This can be attributed to the higher electrocatalytic activity of the C_{60}-MWCNT film on the electrochemistry of Hb than that of the MWCNT film, caused by the more favorable electrochemical environment for Hb in the electrode double layer. In addition, the more facile adsorption of Hb onto the C_{60}-MWCNT film may also be part of the explanation.

The Hb adsorption onto C_{60}-MWCNT and MWCNT films was investigated by recording CVs continuously as a function of time. Upon immersion of a C_{60}-MWCNT film electrode in a Hb solution, the cathodic peak current increased in parallel with the scan time and leveled off to a rather stable level (curve a of Figure 2). This suggests a gradual increase in the amount of Hb adsorbed on the electrode, followed by saturation. In contrast, although the MWCNT film electrode, with the same electrolyte solution as for the C_{60}-MWCNT film electrode, initially shows a higher cathodic peak current, this decreased rapidly over time (curve b of Figure 2), indicating desorption of Hb from the electrode. It appears that a more stable adsorption of Hb on C_{60}-MWCNT films is enabled by the presence of C_{60}.

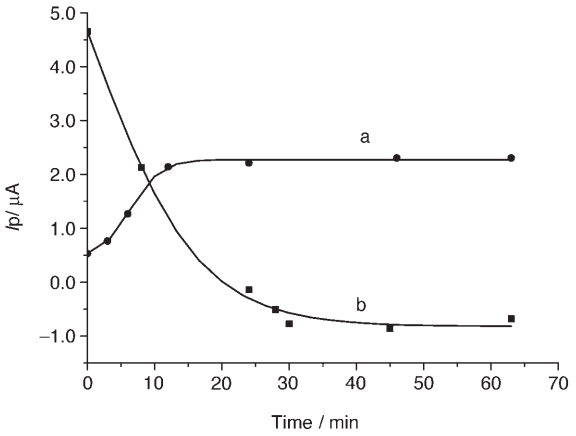

Figure 2. Relationship between cathodic peak current of Hb and CV scanning time for a C_{60}-MWCNT film electrode (a) and a MWCNT film electrode (b) in 5×10^{-5} M Hb phosphate buffer solution. Scan rate: 0.01 V s^{-1}.

The stability of Hb adsorption on the C_{60}-MWCNT film was verified further. After the CV response of the C_{60}-MWCNT film electrode in Hb solution reached a steady state, the Hb/C_{60}-MWCNT film electrode was transferred into a Hb-free phosphate buffer solution and the CV scans were continued. The scan rate was increased from 1 to 10 mV s^{-1} by intervals of 1 mV s^{-1}, and subsequently from 10 to 130 mV s^{-1} by intervals of 20 mV s^{-1}. After these repeated potential scans, we analyzed the CV of the film at the scan rate of 10 mV s^{-1}. The peak current I_p decreased by about only 1.8% relative to that before the repeated potential scans. Furthermore, upon storage of this Hb/C_{60}-MWCNT film in air for about 10 days, no change in its electrochemical behavior occurred and the I_p decreased by about only 1.2%.

Kinetic characteristics of the Hb/C_{60}-MWCNT film electrode: As shown in the inset of Figure 3, the increasing potential scan rate influences the redox behavior of the Hb/C_{60}-MWCNT film electrode by increasing the peak current as well as the peak separation ΔEp. The corresponding scan-rate-dependent data are shown more clearly in Figures 3 and 4, respectively. The linear increase of the cathodic peak current with the scan rate (Figure 3) conforms to the electrochemical characteristic of a thin layer.[27] For a surface process, according to Laviron's equation,[28] the relationship between peak current (I_p) and surface coverage (Γ) is

$$I_p = \frac{n^2F^2\nu A\Gamma}{4RT} = \frac{nFQ\nu}{4RT} \quad (1)$$

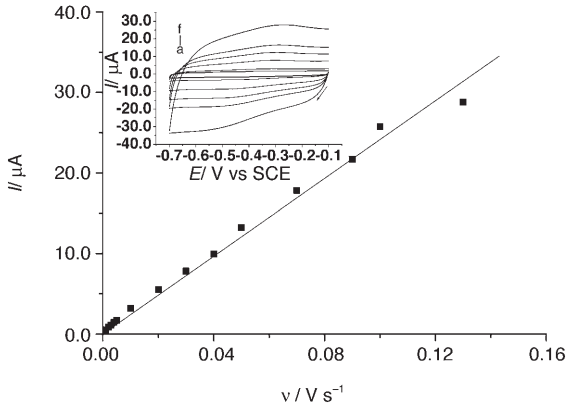

Figure 3. Relationship between scan rate and cathodic peak current for a Hb/C_{60}-MWCNT film electrode in pH 7.0 phosphate buffer solution. Inset: Cyclic voltammograms for Hb/C_{60}-MWCNT films in pH 7.0 phosphate buffer solution at scan rates of (a) 0.005, (b) 0.01, (c) 0.03, (d) 0.05, (e) 0.07, and (f) 0.013 $V s^{-1}$.

in which n is the number of electrons transferred, Q is the amount of charge, A is electrode area ($A = 7.06 \times 10^{-2}$ cm^2 for a flat surface, but is unknown for the C_{60}-MWCNT surface), and F is the Faraday constant. From the CV curves in the inset of Figure 3, Q was calculated to be 4.57×10^{-6} C after background correction. From this, the average surface concentration (Γ) of Hb is estimated to be about $3.63 \times 10^{-9} \pm 7.3 \times 10^{-11}$ $mol\,cm^{-2}$ if a flat surface of C_{60}-MWCNT is assumed. Although the "flat surface" assumption is not justified, it provides a good starting point to address the interfacial electron transfer.

If the scan rate is higher than 0.03 $V s^{-1}$, as shown in Figure 4, the wave shapes are distorted severely and the

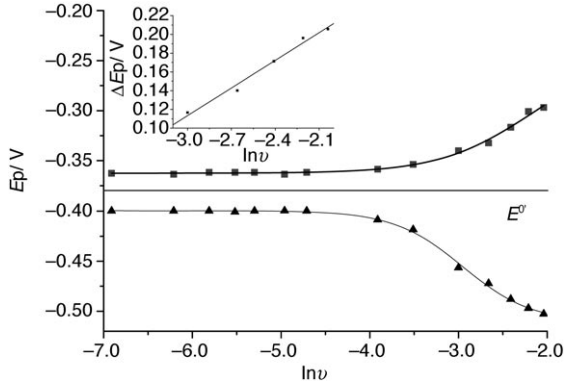

Figure 4. Semilogarithmic dependence of cathodic peak potential (▲), anodic peak potential (■), and scan rate for a Hb/C_{60}-MWCNT film electrode in pH 7.0 phosphate buffer solution. Inset: plot of ΔE_p against $\ln \nu$.

peak separation starts to increase. This indicates that the electrode reaction becomes electrochemically irreversible at higher scan rates. For an irreversible electrode reaction, the relationship between peak potentials and the scan rate follows Laviron's equations:[28,29]

$$E_{pc} = E^{0\prime} - \frac{RT}{\alpha nF}\ln\frac{RTk_s}{\alpha nF} - \frac{RT}{\alpha nF}\ln\nu \quad (2)$$

$$E_{pa} = E^{0\prime} + \frac{RT}{(1-\alpha)nF}\ln\frac{RTk_s}{(1-\alpha)nF} + \frac{RT}{(1-\alpha)nF}\ln\nu \quad (3)$$

According to the above equations, we obtained:

$$\Delta E_p = \frac{RT}{(1-\alpha)\alpha nF}[\alpha\ln(1-\alpha) + (1-\alpha)\ln\alpha - \ln\frac{RT}{nF} - \ln k_s] + \frac{RT}{(1-\alpha)\alpha nF}\ln\nu \quad (4)$$

Here, α is the electron-transfer coefficient, k_s is the standard rate constant of the electrode reaction, ν is the scan rate, and $E^{0\prime}$ is the formal potential. Figure 4 shows the plot of E_p versus $\ln\nu$ of the Hb/C_{60}-MWCNT film in pH 7.0 phosphate buffer solution. The $E^{0\prime}$ (−0.38 V) could be estimated as the midpoint between the cathodic and the anodic peak potentials at low scan rate. At high scan rate, the plots of Ep versus $\ln\nu$ are linear. The equations of the straight line are:

$$E_{pc} = -0.605 - 0.0496\ln\nu \quad (5)$$

$$E_{pa} = -0.197 + 0.0488\ln\nu \quad (6)$$

From $\Delta E_p \sim \ln\nu$ (as shown in the inset of Figure 4), according to Equations (2) and (5), α was estimated to be 0.52 and k_s to be 0.39 s^{-1}. From Equations (3) and (6), the values of α and k_s were obtained as 0.47 and 0.40 s^{-1} at 25 °C, respectively. These similar electron-transfer coefficients and reaction rate constants suggest that the rate-determining step of the reduction and reoxidation processes might be the same for Hb and the electrode through C_{60}-MWCNT.

For comparison, the same measurements were also conducted for Hb in a MWCNT film. From the results summarized in Table 1 for the reduction step, the value of k_s for

Table 1. Electrochemical parameters of Hb in C_{60}-MWCNT film and MWCNT film, respectively.

Film	ΔE_p [mV]	α[a]	k_s [s^{-1}][a]
C_{60}-MWCNT	60	0.52	0.39
MWCNT	71	0.24	0.03

[a] For the reduction steps.

C_{60}-MWCNT films (0.39 s^{-1}) is more than one order of magnitude greater than that for MWCNT films (0.03 s^{-1}), suggesting that the C_{60}-MWCNT films are much more effective in facilitating the direct electron transfer of Hb than the bare MWCNT films. The faster electron-transfer kinetics in the C_{60}-MWCNT nanocomposite must be due to the fine dispersion of C_{60} on the MWCNT surfaces. We argue that C_{60} plays an electron-mediator role interfacing Hb and MWCNT. C_{60} is an excellent electron acceptor and its conjugation with MWCNT forms an interesting heterostructure. Such a heterostructure could act as an electron buffer for fa-

cilitating electron transfer. In fact, the electron-mediator role of C_{60} has been reported previously,[30] although here it is immobilized on the MWCNT surfaces. Perhaps equally important, the adsorbed C_{60} may serve as docking sites for Hb because of the affinity of Hb for fullerenes.[23] The C_{60}-MWCNT conjugate may be configured in such a way that permits the proximity of C_{60} to the redox center of Hb, and this too would drastically enhance the electron-transfer rate.

We next examined the effect of the pH value of the supporting electrolyte on the peak potentials of Hb in the C_{60}-MWCNT film and the results are shown in Figure 5. With

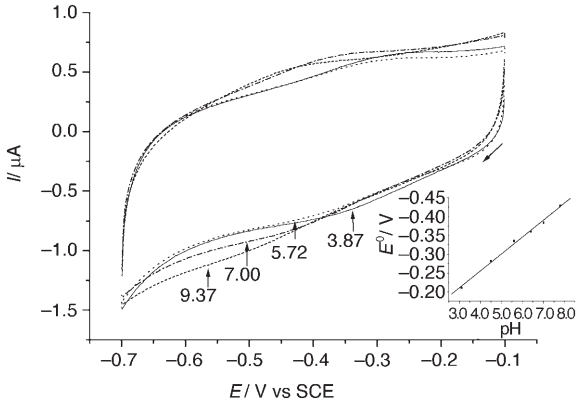

Figure 5. Cyclic voltammograms of a C_{60}-MWCNT film electrode in solutions of different pH (pH values are indicated by the arrows) containing 5×10^{-5} M Hb. Scan rate: 0.01 V s^{-1}. Inset: plot of potential versus pH value.

the increase in pH value from 3.5 to 9.5, the formal potential $E^{0\prime}$ of Hb in the C_{60}-MWCNT film shifts linearly in the negative direction. The slope of the plot of $E^{0\prime}$ versus pH was -48 mV pH^{-1} (inset of Figure 5), which is close to the theoretical value of -58 mV pH^{-1} at 20 °C for reversible electron transfer coupled by single-proton transfer.[31,32]

Electrocatalysis of the Hb/C_{60}-MWCNT electrode for the reduction of oxygen: The stable and redox-active Hb/C_{60}-MWCNT film electrode described above offers good opportunities to explore its potential applications. To this end, we studied the electrocatalytic properties of this nanocomposite film electrode through the reduction of oxygen present in the electrolyte solution. The Hb/C_{60}-MWCNT film electrode was immersed in a phosphate buffer solution containing a predetermined amount of O_2 (introduced by injecting a known amount of air into the electrochemical cell using a syringe). Two representative CVs are shown as curve b (10 mL) and curve c (20 mL) in Figure 6. Relative to the CV in the absence of O_2 (curve a), the Hb reduction peaks in both curves were increased considerably. The reduction peak was accompanied by a decrease in the reoxidation peak during the scan reversal. Thus, the electrode reaction is characteristic of an ErCi' mechanism:[33]

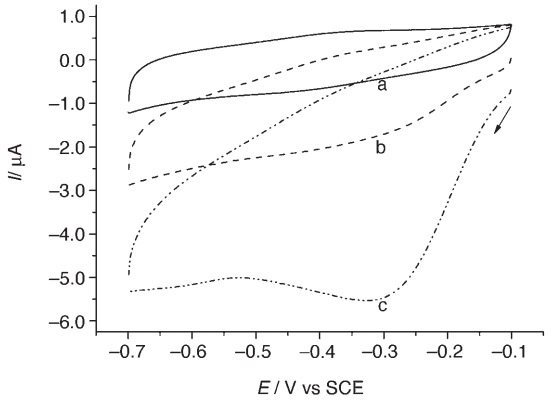

Figure 6. Cyclic voltammograms of Hb/C_{60}-MWCNT films in pH 7.0 phosphate buffer solution containing (a) no air, (b) 10 mL air, and (c) 20 mL air. Scan rate: 0.01 V s^{-1}.

$$\mathrm{Hb(Fe^{III})/C_{60}\text{-}MWCNT}+\mathrm{H^+}+\mathrm{e^-}\rightarrow \mathrm{Hb(Fe^{II})/C_{60}\text{-}MWCNT} \quad (7)$$

$$\mathrm{O_2}+\mathrm{Hb(Fe^{II})/C_{60}\text{-}MWCNT}\rightarrow \mathrm{Hb(Fe^{III})/C_{60}\text{-}MWCNT}+\mathrm{H^+}+\mathrm{H_2O} \quad (8)$$

in which Hb(Fe^{III})/C_{60}-MWCNT and Hb(Fe^{II}) denote the oxidized and reduced forms of Hb in C_{60}-MWCNT film, respectively.[34] These reactions also explain the pH effect on the peak potential.

Spectral and microscopic characterizations: We further examined the stability of Hb adsorbed on the C_{60}-MWCNT film by using spectral and microscopic techniques. In the IR spectrum shown in Figure 7, two main amide bands, in the ranges of 1700–1600 and 1600–1500 cm^{-1}, were observed from Hb in KBr pellet (curve a). The former (1657 cm^{-1}, amide I band) is caused by C=O stretching vibrations of peptide linkages in the Hb backbone, and the latter (1533 cm^{-1}, amide II band) results from a combination of N–H in-plane bending and C–N stretching of the peptide groups.[35] The Hb/C_{60}-MWCNT film also showed two main

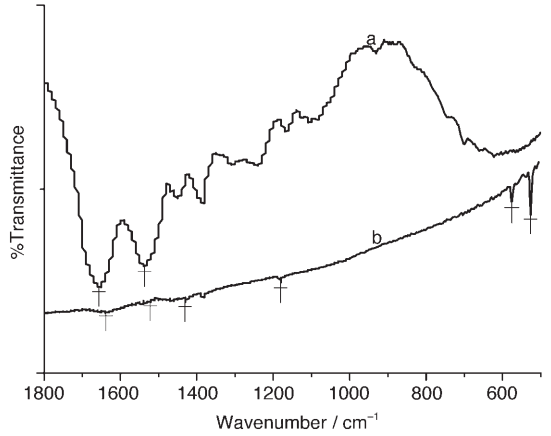

Figure 7. FTIR spectra (KBr pellet) of (a) Hb and (b) Hb/C_{60}-MWCNT films.

amide bands (1637 and 1531 cm^{-1}, respectively) (curve b), which suggests that Hb in C_{60}-MWCNT film does not perturb the Hb conformations drastically. The relative shifts of the peaks are ascribable to the interaction between Hb and the C_{60}-MWCNT nanocomposite, and this explains why the presence of C_{60} significantly enhances the Hb adsorption onto the MWCNTs. Moreover, the bands at 576, 527, 1182, and 1428 cm^{-1} are the characteristic bands of C_{60} on MWCNTs.[24]

An SEM image of the Hb/C_{60}-MWCNT film after redox scans is also shown in Figure 8. Many MWCNTs form bundles with diameters of 10–50 nm. The nanoparticles on the MWCNT surfaces may be attributed to the adsorbed Hb because the size of C_{60} domains on the MWCNTs are smaller, according to our early work.[24]

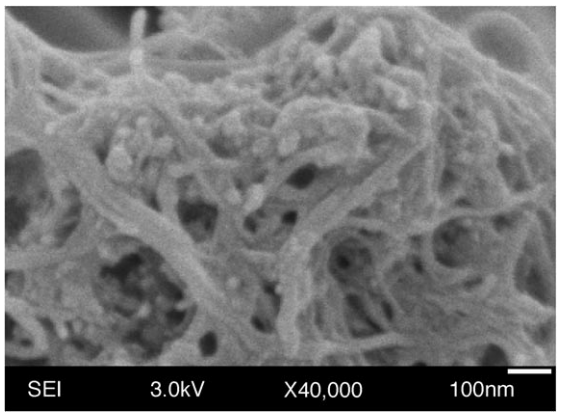

Figure 8. SEM image of a Hb-C_{60}-MWNT composite film.

Summary and Conclusions

We have demonstrated that C_{60}-MWCNT films as a novel nanocomposite material can facilitate the direct electron transfer of Hb much more effectively than bare MWCNT films. Specifically, the heterogeneous electron-transfer rate constant k_s of Hb is 0.39 s^{-1} on the C_{60}-MWCNT film, whereas it is only 0.03 s^{-1} on the MWCNT film under our experimental conditions. We attribute the faster electron-transfer kinetics on the C_{60}-MWCNT film to the roles of electron mediator and protein docking site played by C_{60}, which is finely dispersed on the MWCNT surfaces. In this way, Hb can transfer electrons to and from the electrode more easily through C_{60} in the C_{60}-MWCNT nanocomposite film. In addition, we have shown that the electrode reaction of Hb on the C_{60}-MWCNT film is a single-proton electrode-reaction process. Remarkably, the Hb/C_{60}-MWCNT film is physically, chemically, and electrochemically stable. Finally, the native structure of Hb in the Hb/C_{60}-MWCNT film is preserved and the nanocomposite film displays an excellent electrocatalytic activity for the reduction of O_2. Our studies are the first to suggest the enhancement of the electron-transfer kinetics by using a nanocomposite film, which combines two novel forms of carbon; C_{60} and CNTs. The results presented here should facilitate the development of new biochemical sensors.

Experimental Section

C_{60} (>99.9%) was purchased from Peking University and was used as received. Multiple-walled carbon nanotubes (MWCNTs) from Helix Material Solutions were purified further prior to use by magnetic stirring in concentrated nitric acid for 12 h. Toluene ($C_6H_5CH_3$) (Park Co., Dublin, Ireland) was dried with sodium, refluxed for 6 h, and then distilled. The purified toluene was stored in the presence of sodium. Hemoglobin was from Sigma. Other reagents used in the experiments were of analytical grade.

The C_{60}-MWCNT film electrode was prepared as described previously.[24] Briefly, purified MWCNTs and C_{60} (MWCNTs/C_{60}=2:1) with a total amount of about 1 mg were dispersed in 10 mL toluene in an ultrasound bath for 30 min to give a 0.1 mg mL^{-1} suspension. A volume of 15 μL of the suspension was cast directly on a glassy carbon (GC) electrode surface and the solvent was allowed to evaporate at RT. This C_{60}-MWCNT film electrode was subjected to potential scanning in acetonitrile solution containing 0.1 M tetrabutylammonium hexafluorophosphate ($TBAPF_6$) between 0.0 and −2.0 V (vs Ag/AgCl) to obtain reversible multiple-step electron-transfer similar to that of C_{60} dissolved in an organic solution, but with superposed electrochemical features of bare MWCNTs.[24] The resultant C_{60}-MWCNT film electrode was then washed with acetonitrile several times to remove the electrolytes, and then dried at RT.

Cyclic voltammetry (CV) (CHI610B, Austin, USA) was performed with a three-electrode configuration. The C_{60}-MWCNT or MWCNT film on the GC electrode was used as the working electrode. A Pt-wire electrode served as the auxiliary electrode, and a saturated calomel electrode (SCE) was used as the reference. All electrochemical experiments were performed in a high purity N_2 atmosphere at ambient temperature.

FTIR spectra were measured by using an AVATAR 360 FTIR spectroscope (Nicolet, USA). Scanning electron microscopy (SEM) was performed by using a KYKY2000 SEM instrument in the secondary electron emission mode.

Acknowledgement

This work was financially supported by the National Natural Science Foundation of China (20473014), the Major State Basic Research Development Programs (2004CB719903) and NNSFC-RGC administrated by the UGC of Hong Kong (N HKUST604/04).

[1] H. Tokuyama, S. Yamago, E. Nakumura, T. Shiraki, Y. Sugiura, *J. Am. Chem. Soc.* **1993**, *115*, 7918–7919.
[2] S. H. Friedman, D. L. Decamp, R. P. Sijbesmaa, G. Srdanov, F. Wudl, G. L. Kenyon, *J. Am. Chem. Soc.* **1993**, *115*, 6506–6509.
[3] R. Sijbesma, G. Srdanov, F. Wudl, J. A. Castoro, C. Wilkins, S. H. Friedman, D. L. Decamp, G. L. Kenyon, *J. Am. Chem. Soc.* **1993**, *115*, 6510–6512.
[4] L. Z. Fan, S. F. Yang, S. H. Yang, *J. Electroanal. Chem.* **2005**, *574*, 273–283.
[5] T. DaRos, M. Prato, *Chem. Commun.* **1999**, 663–669.
[6] J. Kong, N. R. Franklin, C. Zhou, M. G. Chapline, S. Peng, K. Cho, H. Dai, *Science* **2000**, *287*, 622–625.
[7] J. Kong, M. G. Chapline, H. Dai, *Adv. Mater.* **2001**, *13*, 1384–1386.
[8] R. J. Chen, S. Bangsaruntip, K. A. Drouvalakis, N. W. S. Kam, M. Shim, Y. Li, W. Kim, P. J. Utz, H. Dai, *Proc. Natl. Acad. Sci. USA* **2003**, *100*, 4984–4989.
[9] J. Wang, M. Musameh, Y. Lin, *J. Am. Chem. Soc.* **2003**, *125*, 2408–2409.
[10] J. Wang, M. Musameh, *Anal. Chem.* **2003**, *75*, 2075–2079.

[11] S. J. Tans, A. R. M. Verschueren, C. Dekker, *Nature* **1998**, *393*, 49–52.
[12] H. Dai, J. H. Hafner, A. G. Rinzler, D. T. Colbert, R. E. Smalley, *Nature* **1996**, *384*, 147–150.
[13] S. S. Wong, J. D. Hafner, P. T. Lansbury, C. M. Lieber, *J. Am. Chem. Soc.* **1998**, *120*, 603–604.
[14] P. J. Britto, K. S. V. Santhanam, P. M. Ajayan, *Bioelectrochem. Bioenerg* **1996**, *41*, 121–125.
[15] N. Mano, A. Heller, *Anal. Chem.* **2005**, *77*, 729–732.
[16] N. S. Lawrence, R. P. Deo, J. Wang, *Anal. Chem.* **2004**, *76*, 3735–3739.
[17] K. M. Faulkner, C. Bonaventura, A. L. Crumbliss, *J. Biol. Chem.* **1995**, *270*, 13604–13610.
[18] C. Fan, I. Suzuki, Q. Chen, G. Li, J. I. Anzai, *Anal. Lett.* **2000**, *33*, 2631–2633.
[19] J. Yu, H. Ju, *Anal. Chem.* **1988**, *60*, 2263–2268.
[20] H. Sun, N. Hu, H. Ma, *Electroanalysis* **2000**, *11*, 1064–1070.
[21] X. Han, W. Huang, J. Jia, S. Dong, E. Wang, *Biosens. Bioelectron.* **2002**, *17*, 741–746.
[22] P. L. Yang, Q. Zhao, Z. N. Gu, Q. K. Zhuang, *Electroanalysis* **2004**, *15*, 97–100.
[23] M. X. Li, M. T. Xu, N. Q. Li, Z. N. Gu, X. H. Zhou, *J. Phys. Chem. B* **2002**, *106*, 4197–4202.
[24] H. Zhang, L. Z. Fan, Y. P. Fang, S. H. Yang, *Chem. Phys. Lett.* **2005**, *413*, 346–350.
[25] A. Szucs, A. Loix, J. B. Nagy, L. Lamberts, *Electroanal. Chem.* **1995**, *397*, 191–203.
[26] A. Szucs, A. Loix, J. B. Nagy, L. Lamberts, *Electroanal. Chem.* **1996**, *402*, 137–148.
[27] A. J. Bard, L. R. Faulkner, *Electrochemical Methods*, Wiley, New York, **1980**, p. 522.
[28] E. Laviron, *J. Electroanal. Chem.* **1974**, *52*, 355–393.
[29] E. Laviron, *J. Electroanal. Chem.* **1979**, *101*, 19–28.
[30] K. Hwang, D. Mauzerall, *J. Am. Chem. Soc.* **1992**, *114*, 9705–9706.
[31] L. Meites, *Polarographic Techniques*, 2nd ed., Wiley, New York, **1965**.
[32] M. M. Baizer, H. Lund, *Organic Electrochemistry*, Marcel Dekker, New York, **1983**, p. 507.
[33] A. J. Bard, L. R. Faulkner, *Electrochemical Methods: Fundamentals and Applications*, Wiley, New York, **2001**.
[34] L. Wang, J. X. Wang, F. M. Zhou, *Electroanalysis* **2004**, *15*, 627–632.
[35] X. Chen, H. Xie, J. Kong, J. Deng, *Biosens. Bioelectron.* **2001**, *16*, 115–120.

Received: January 14, 2006
Revised: March 17, 2006
Published online: June 28, 2006

